 CMES, vol.50, no.2, pp.97-114, 2009

Numerical Modelling of Electromagnetic Wave Propagation by Meshless Local Petrov-Galerkin Formulations

Delfim Soares Jr.[1]

Abstract: In this work, meshless methods based on the local Petrov-Galerkin (MLPG) approach are presented to analyse electromagnetic wave propagation problems. Formulations adopting the Heaviside step function and the Gaussian weight function as the test functions in the local weak form are considered. The moving least square (MLS) method is used to approximate the physical quantities in the local integral equations. After spatial discretization is carried out, a system of ordinary differential equations of second order is obtained. This system is solved in the time-domain by the Houbolt's method, allowing the computation of the so-called primary fields (either the electric or the magnetic field can be selected as the primary field; the complementary field is here referred to as secondary field). The secondary field is obtained following Maxwell's equations, i.e., considering space derivatives of the primary field and time integration procedures. This methodology is more efficient and flexible since fewer systems of equations must be solved along the analysis. At the end of the paper, numerical applications illustrate the accuracy and potentialities of the proposed techniques.

Keywords: Meshless Local Petrov-Garlekin; Moving Least Square Interpolation; Maxwell's Equations; Wave Propagation Problems; Time-Domain Analysis; Electromagnetic Fields.

1 Introduction

In spite of the great success of the finite and boundary element methods as effective numerical tools for the solution of boundary value problems on complex domains, there is still a growing interest in the development of new advanced methods. Nowadays, many meshless formulations are becoming popular, due to their high adaptivity and to their low-cost effort to prepare input data (meshless methods

[1] Faculty of Engineering, Federal University of Juiz de Fora, Cidade Universitária, CEP 36036-330, Juiz de Fora, MG, Brazil. Tel: +55 32 2102-3468; E-mail: delfim.soares@ufjf.edu.br

were essentially stimulated by difficulties related to mesh generation). In addition, the need for flexibility in the selection of approximating functions (*e.g.*, the flexibility to use non-polynomial approximating functions) has played a significant role in the development of meshless methods (many meshless approximations give continuous variation of the first or higher order derivatives of a primitive function in counterpart to classical polynomial approximation where secondary fields have a jump on the interface of elements. Therefore, meshless approximations are leading to more accurate results in many cases).

A variety of meshless methods has been proposed along the last decade to analyze electromagnetic fields. Mostly, these formulations have been applied to the computation of permanent fields: Marechal (1998) and Ho et al. (2001), for instance, employed some meshless methods to compute (and post-treat) electromagnetic fields; Li and Lee (2006) presented an adaptive meshless method for magnetic field computation; Lee et al. (2006) compared two meshless methods (point collocation and Galerkin methods) to analyze Poisson-like problems with discontinuities at material interfaces; Guimaraes et al. (2007) developed a meshless method for electromagnetic field computation based on the multiquadric interpolation technique; etc. Most of the works presented so far, to compute electromagnetic fields, employs the so-called Element Free Galerking (EFG) method. In this context, Clingoski et al. (1998) are among the firsts to apply the EFG method to analyze electrostatic fields; latter on, Xuan et al. (2004) and Parreira et al. (2006) extended its application to the analysis of some quasi-static and three-dimensional fields, respectively, and Louai et al. (2007) and Marques et al. (2007) presented some further advancements on the EFG methodology, considering Poisson-like problems. Taking into account Meshless Local Petrov-Galerking (MLPG) formulations, the works of Viana et al. (2004), Ni et al. (2004) and Zhao and Nie (2008) are among the few related to the analysis of permanent electromagnetic fields.

Very recently, meshless methods began to be applied to the analysis of transient electromagnetic fields. In this context, Reutskiy and Tirozzi (2004) presented a formulation for the scattering analysis from inhomogeneous bodies; Young et al. (2005) and Lai et al. (2008) described meshless methods based on radial basis functions for transient electromagnetic computations; and Ala et al. (2007) and Francomano et al. (2009) reformulated the meshless Smoothed Particle Hydrodynamics method for solving the time domain Maxwell's equations. The Element Free Galerking method was applied by Liu et al. (2007) and Manzin and Bottauscio (2008) to analyze electromagnetic scattering problems. Considering Meshless Local Petrov-Galerkin formulations applied to the computation of transient electromagnetic fields, as far as the author is concerned, this is the first work on the topic.

In the present work, two MLPG formulations are presented to analyze electromagnetic wave propagation problems in the time domain (a few key references to the original papers where the MLPG method was presented can be given by: Atluri and Zhu, 1998 and 2000; Atluri and Shen, 2002; and Atluri et al., 2003 and 2004. References concerning the numerical modelling of electromagnetic waves can be given by: Soares and Vinagre, 2008; and Soares, 2008 and 2009). In the first formulation, Heaviside step functions are selected as the test functions, whereas, in the second formulation, Gaussian weight functions are the selected test functions. Two-dimensional problems are focused here and the spatial variation of the incognita field is approximated by the moving least-square (MLS) scheme. Once the spatial discretization is carried out, a time domain system of second order ordinary differential equations arises, which is treated here by the Houbolt's method. This methodology allows the computation of the primary electromagnetic field. This primary field can be either the electric or the magnetic field (the selection is considered taking into account the characteristics of the problem to model). Once the so-called primary field is evaluated (analyzing wave propagation problems), the secondary field (magnetic or electric field – the one which complements the primary field) is computed directly, considering Maxwell's equations.

The above-described procedure aims to be more efficient, since fewer systems of equations (just the systems related to the primary field) need to be solved at each time step of the analysis. Moreover, since just one electromagnetic field (primary field) is modelled, more flexible and easier to implement simulations take place. One should notice that, following Maxwell's equations, spatial derivatives of the primary field are necessary in order to compute the secondary field. Since meshless methods provide a continuous variation of these derivatives, more accurate results are expected considering these formulations.

It is important to observe that, taking into account some finite element procedures, spurious or non-physical solutions may arise once the divergence conditions are not satisfied (Jin, 2002). This is due to the fact that, in these finite element procedures, only the interpolation or expansion functions (not their derivatives) are forced to be continuous. There are several approaches that can be used to eliminate the spurious solutions. One approach calls for the use of interpolation functions that have continuous derivatives even on element boundaries (i.e., C^1 functions; in counter part to the usual C^0 interpolation functions). C^1 functions are usually more complicated and thus more difficult to implement in finite element analysis and, for this reason, this approach has not gained any popularity to date (Jin, 2002). The MLPG formulations presented here, on the other hand, are based on C^1 continuity.

2 Governing equations

Maxwell's equations in differential form can be written as follows:

$$e_{ijk}E_{k,j} = -\dot{B}_i \tag{1a}$$

$$e_{ijk}H_{k,j} = \dot{D}_i + J_i \tag{1b}$$

$$D_{i,i} = \rho \tag{1c}$$

$$B_{i,i} = 0 \tag{1d}$$

where indicial notation for Cartesian axes is considered and e_{ijk} stands for the permutation symbol (also known as alternator tensor). Inferior commas and overdots indicate partial space and time derivatives, respectively (i.e., $V_{i,j} = \partial V_i/\partial x_j$ and $\dot{V}_i = \partial V_i/\partial t$, where $V_i(X,t)$ stands for a generic vector field representation and X and t denote its spatial and temporal arguments, respectively).

In equations (1), E_i and H_i are the electric and magnetic field intensity components, respectively; D_i and B_i represent the electric and magnetic flux density, respectively; and J_i and ρ stand for the electric current and electric charge density, respectively. The constitutive relations between the field quantities are specified as follows:

$$D_i = \varepsilon E_i \tag{2a}$$

$$B_i = \mu H_i \tag{2b}$$

$$J_i = \sigma E_i \tag{2c}$$

where the parameters ε, μ and σ denote, respectively, the permittivity, permeability and conductivity of the medium.

Combining equations (1) and (2), vectorial wave equations describing the electric and the magnetic field can be obtained, as is indicated below:

$$e_{mni}(\mu^{-1}e_{ijk}E_{k,j})_{,n} + \varepsilon \ddot{E}_m = -\dot{J}_m \tag{3a}$$

$$e_{mni}(\varepsilon^{-1}e_{ijk}H_{k,j})_{,n} + \mu \ddot{H}_m = e_{mni}(\varepsilon^{-1}J_i)_{,n} \tag{3b}$$

where the wave propagation velocity of the medium is specified as $c = (\varepsilon\mu)^{-1/2}$.

Taking into account two-dimensional applications, equations (3) can be simplified and written in a unique general form:

$$(\kappa^{-1}\phi_{,i})_{,i} - \nu\ddot{\phi} = \gamma \tag{4}$$

where ϕ is a generic representation for an electric (E_k) or magnetic (H_k) field intensity component (e.g., $i = 1, 2$ and $k = 3$) and γ stands for a generic source term. κ and ν represent μ or ε, according to the case of analysis.

Once the governing differential equation is established, temporal and spatial boundary conditions must be defined. The boundary conditions for the model in focus are:

(i) Spatial Boundary Conditions ($t \geq 0$, $X \in \Gamma$ where $\Gamma = \Gamma_\phi \cup \Gamma_\theta$):

$$\phi = \bar{\phi} \text{ for } X \in \Gamma_\phi \tag{5a}$$

$$\theta = \phi_{,i} n_i = \bar{\theta} \text{ for } X \in \Gamma_\theta \tag{5b}$$

(ii) Temporal Boundary Conditions ($t = 0$, $X \in \Omega$):

$$\phi = \bar{\phi}^0 \tag{5c}$$

$$\dot{\phi} = \dot{\bar{\phi}}^0 \tag{5d}$$

where equations (5c) and (5d) stand for the initial conditions of the problem, equation (5a) stands for essential (or Dirichlet) boundary conditions and equation (5b) stands for natural (or Neumann) boundary conditions (n_i represents an outward unit vector normal to the boundary). In equations (5), overbars indicate prescribed values and the boundary of the model is denoted by Γ, whereas the domain is denoted by Ω.

3 Spatial discretization

In general, a meshless method uses a local approximation to represent the trial function in terms of nodal unknowns which are either the nodal values of real field variables or fictitious nodal unknowns at some randomly located nodes. The moving least squares (MLS) approximation may be considered as one of such schemes, and it is used here.

Consider a sub-domain Ω_x, the neighbourhood of a point X and denoted as the domain of definition of the MLS approximation for the trial function at X, which is located in the problem domain Ω (see Fig.1). To approximate the distribution of function ϕ in Ω_x, over a number of randomly located nodes, the MLS approximation of ϕ can be defined by (Atluri and Shen, 2002; Atluri, 2004):

$$\phi(X,t) \approx \sum_{a=1}^{N} \eta^a(X) \hat{\phi}^a(t) \tag{6}$$

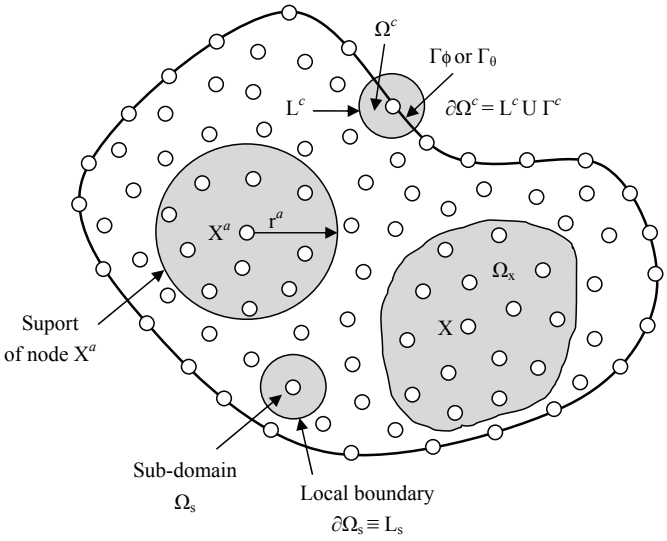

Figure 1: Local boundaries, sub-domains and domain of definition of the MLS approximation for the trial function at node X.

where $\hat{\phi}$ is the fictitious nodal value of ϕ and N is the number of points in the sub-domain Ω_x. The shape matrix $\mathbf{N}^T(X) = [\eta^1(X), \eta^2(X), \ldots, \eta^N(X)]$ is computed by:

$$\mathbf{N}^T(X) = \mathbf{p}^T(X)\mathbf{A}^{-1}(X)\mathbf{B}(X) \tag{7}$$

where

$$\mathbf{A}(X) = \sum_{a=1}^{N} w^a(X)\mathbf{p}(X^a)\mathbf{p}^T(X^a) \tag{8a}$$

$$\mathbf{B}(X) = [w^1(X)\mathbf{p}(X^1), w^2(X)\mathbf{p}(X^2), ..., w^N(X)\mathbf{p}(X^N)] \tag{8b}$$

and $\mathbf{p}^T(X) = [p_1(X), p_2(X), \ldots, p_m(X)]$ is a complete monomial basis of order M. $w^a(X)$ is the weight function associated with node A. The gaussian weight function is adopted here, and it is given by:

$$w^a(X) = \frac{\exp[-(d_a/c_a)^{2k}] - \exp[-(r_a/c_a)^{2k}]}{1 - \exp[-(r_a/c_a)^{2k}]}(1 - H[d_a - r_a]) \tag{9}$$

where $d_a = ||X - X^a||$ is the distance between the sampling point X and node X^a, c_a is a constant controlling the shape of the weight function and r_a is the radius

of the circular support of the weight function. The Heaviside unit step function is defined as $H[z] = 1$ for $z > 0$ and $H[z] = 0$ for $z \leq 0$. The size of the weight function support should be large enough to have a sufficient number of nodes covered in the domain of definition to ensure the regularity of matrix $\mathbf{A}$.

Instead of writing the global weak-form for the governing equations described in section 2, the MLPG method constructs a weak-form over local fictitious sub-domains, such as Ω_s, which is a small region taken for each node inside the global domain (see Fig.1). The local sub-domains overlap each other, and cover the whole global domain Ω. The geometrical shape and size of local sub-domains can be arbitrary. In the present paper, the local sub-domains are taken to be of circular shape. The local weak-form of the governing equations (4) can be written as:

$$\int_{\partial\Omega_s} \varphi\, \kappa^{-1} \theta\, d\Gamma - \int_{\Omega_s} \varphi_{,i}\, \kappa^{-1} \phi_{,i} d\Omega + \int_{\Omega_s} \varphi\, (\gamma - \nu\, \ddot{\phi})\, d\Omega + \lambda \int_{\Gamma_{s\phi}} \varphi\, (\phi - \bar{\phi})\, d\Gamma = 0 \quad (10)$$

where ϕ is a test function and λ is a penalty parameter, which is introduced here in order to impose essential prescribed boundary conditions in an integral form. In equation (10), $\partial\Omega_s$ is the boundary of the local sub-domain, which consists of three parts, in general: $\partial\Omega_s = L_s \cup \Gamma_{s\theta} \cup \Gamma_{s\phi}$. Here, L_s is the local boundary that is totally inside the global domain, $\Gamma_{s\theta}$ is the part of the local boundary which coincides with the global natural boundary, i.e., $\Gamma_{s\theta} = \partial\Omega_s \cap \Gamma_\theta$, and similarly $\Gamma_{s\phi}$ is the part of the local boundary that coincides with the global essential boundary, i.e., $\Gamma_{s\phi} = \partial\Omega_s \cap \Gamma_\phi$ (see Fig.1).

Equation (10) can be rewritten by taking into account approximation (6) and by defining the local integral sub-domain as the circle Ω^c, centred at the node $X^c$and described by radius r_c. The expressions that arise, considering the test functions specified as $\varphi = 1 - H(d_c - r_c)$ (Heaviside step function) or as $\varphi = w^c$ (Gaussian weight function), are given, respectively, by:

$$\sum_{a=1}^{N} \left[\left(\int_{\Omega^c} \nu \eta^a d\Omega \right) \ddot{\hat{\phi}}^a - \left(\lambda \int_{\Gamma_\phi^c} \eta^a d\Gamma + \int_{L^c + \Gamma_\phi^c} \kappa^{-1} n_i \eta^a_{,i} d\Gamma \right) \hat{\phi}^a \right] =$$

$$= \int_{\Gamma_\theta^c} \bar{\theta}\, d\Gamma + \int_{\Omega^c} \gamma d\Omega - \lambda \int_{\Gamma_\phi^c} \bar{\phi} d\Gamma \quad (11a)$$

$$\sum_{a=1}^{N}\left[\left(\int_{\Omega^c} w^c \nu \eta^a d\Omega\right)\ddot{\hat{\phi}}^a - \right.$$

$$\left. -\left(\lambda\int_{\Gamma_\phi^c} w^c \eta^a d\Gamma + \int_{\Gamma_\phi^c} w^c \kappa^{-1} n_i \eta^a_{,i} d\Gamma - \int_{\Omega^c} w^c_{,i} \kappa^{-1} \eta^a_{,i} d\Omega\right)\hat{\phi}^a\right] =$$

$$= \int_{\Gamma_\theta^c} w^c \bar{\theta}\, d\Gamma + \int_{\Omega^c} w^c \gamma d\Omega - \lambda\int_{\Gamma_\phi^c} w^c \bar{\phi} d\Gamma \quad (11b)$$

By collecting all nodal unknown fictitious values $\hat{\phi}^a(t)$ into vector $\hat{\mathbf{\Phi}}$, the system of the discretized equations (11a) or (11b) can be rewritten into matrix form, as follows:

$$\mathbf{M}\ddot{\hat{\mathbf{\Phi}}} + \mathbf{K}\hat{\mathbf{\Phi}} = \mathbf{F} \quad (12)$$

where $\hat{\mathbf{\Phi}}$ is a generic vector describing electric or magnetic field components, $\mathbf{M}$ is the matrix evaluated taking into account the first integral term on the l.h.s. of equations (11); $\mathbf{K}$ is the matrix computed considering the second terms on the l.h.s. of equations (11); and $\mathbf{F}$ is the vector of generalized applied sources, evaluated considering the terms on the r.h.s. of equations (11). Once the second order ordinary differential matrix equation (12) is established, its solution in the time-domain is discussed in the next section, taking into account finite difference procedures.

4 Temporal discretization

The Houbolt's method is considered here to solve the system of second order ordinary differential equations (12) in the time-domain (Houbolt, 1950). It is important to observe that the Houbolt's method provides high-frequency dissipation, eliminating the contribution of spurious modes, which is of great importance considering MLPG formulations, in order to avoid unstable results. In the Houbolt's method, the following finite difference expression is considered in order to approximate $\ddot{\hat{\mathbf{\Phi}}}$ at time t^{n+1}:

$$\ddot{\hat{\mathbf{\Phi}}}^{n+1} = (2\hat{\mathbf{\Phi}}^{n+1} - 5\hat{\mathbf{\Phi}}^{n} + 4\hat{\mathbf{\Phi}}^{n-1} - \hat{\mathbf{\Phi}}^{n-2})/\Delta t^2 \quad (13)$$

where Δt is a selected time-step.

After introducing relation (13) into the system of equations (12), the following system of equations arises, which allows the computation of the fictitious nodal values $\hat{\phi}$ at each time-step:

$$\bar{\mathbf{A}}\hat{\mathbf{\Phi}}^{n+1} = \bar{\mathbf{B}} \quad (14)$$

where $\bar{\mathbf{A}}$ and $\bar{\mathbf{B}}$ are the houlbot's effective matrix and vector, respectively, given by:

$$\bar{\mathbf{A}} = (2/\Delta t^2)\mathbf{M} + \mathbf{K} \tag{15a}$$

$$\bar{\mathbf{B}} = \mathbf{F}^{n+1} + (1/\Delta t^2)\,\mathbf{M}\,(5\hat{\mathbf{\Phi}}^n - 4\hat{\mathbf{\Phi}}^{n-1} + \hat{\mathbf{\Phi}}^{n-2}) \tag{15b}$$

5 Computation of secondary fields

In the present work, instead of analysing both electric and magnetic problems (equations (3a) and (3b)) taking into account equations (4)-(14), just the electric or the magnetic field (the selected field is named here "primary" and the other one is named "secondary") is computed by this procedure. The secondary field is calculated by taking into account equations (1) and (2), i.e., by directly employing Maxwell's equations. Thus, a more efficient procedure is achieved since fewer systems of equations must be solved.

In order to evaluate the secondary field, space derivatives of the primary field are necessary (see equations (1)). Taking into account MLPG formulations, these derivatives can be computed as follows:

$$\phi_{,i}(X,t) \approx \sum_{a=1}^{N} \eta_{,i}^{a}(X)\hat{\phi}^{a}(t) \tag{16}$$

where the derivatives of the shape functions are computed as indicated below:

$$\mathbf{N}_{,i}^{T}(X) = \mathbf{p}_{,i}^{T}(X)\mathbf{A}^{-1}(X)\mathbf{B}(X) + \mathbf{p}^{T}(X)\mathbf{A}_{,i}^{-1}(X)\mathbf{B}(X) + \mathbf{p}^{T}(X)\mathbf{A}^{-1}(X)\mathbf{B}_{,i}(X) \tag{17}$$

with $\mathbf{A}_{,i}^{-1}(X)$ given by $\mathbf{A}_{,i}^{-1}(X) = \mathbf{A}^{-1}(X)\mathbf{A}_{,i}(X)\mathbf{A}^{-1}(X)$.

Once the spatial derivatives of the primary field are computed at the selected nodes, they can be combined regarding equations (1)-(2), obtaining the temporal derivative of the secondary field. In the sequence, this time derivative field can be integrated along time by some simple numerical procedure (such as the trapezoid rule), allowing the final computation of the secondary field.

It is important to highlight that the adopted meshless techniques give continuous variation of the first or higher order derivatives of the primitive function (in counterpart to classical finite element polynomial approximations where secondary fields have a jump on the interface of elements). Therefore, more accurate results are expected regarding the present primary-secondary field approach by these techniques, since proper computation of spatial derivatives plays a crucial role on this methodology.

6 Numerical aspects and applications

Two numerical applications are considered here, illustrating the discussed methodologies. In the first application the electromagnetic wave propagation between two parallel lines of wires is analysed, whereas, in the second application, the behaviour of the electromagnetic fields generated by two cylindrical lines of wires is studied. In the first case, the results obtained by the MLPG formulations are compared to analytical answers, whereas, in the second case, the obtained results are compared to those provided by the boundary element method (BEM). The following nomenclature is adopted here, considering the meshless formulations in focus: (i) MLPG1 denotes the MLPG formulation employing heaviside test functions; (ii) MLPG2 denotes the MLPG formulation that employs the weight functions as the test functions.

In the present work, the radii of the influence domain and of the local sub-domain are set to $\alpha_x d_i^3$ and $\alpha_s d_i^1$, respectively; where d_i^3 and d_i^1 are the distances to the third and first nearest points from node i, respectively. In all the applications that follow, $\alpha_x = 5$ is selected, as well as $\alpha_s = 0.6$ and $\alpha_s = 1.0$ are selected for the MLPG1 and MLPG2 formulations, respectively. The $\mathbf{M}$ matrix is adopted diagonal (it is diagonalized by a row-sum technique), which allows a very efficient time-marching procedure, once the computational cost of the effective vector evaluation is drastically reduced (see equation (15b)). For the computation of the secondary field, the trapezoid rule is employed for time integration.

6.1 Parallel lines of wires

In this sub-section, two parallel lines of wires, carrying opposite time-linear currents, are considered and the electromagnetic field evolution within these lines is analysed. A sketch of the model and the adopted spatial discretization are depicted in Fig.2: 153 nodes are employed in the analyses, in a regular equally spaced 9x17 (vertical and horizontal, respectively) distribution (the geometry of the model is defined by $a = b = 0.0625\,m$ and $L = 2\,m$). The symmetry of the model is taken into account and the spatial discretization is considered only between points A and C. For the temporal discretization, the selected time-step is given by $\Delta t = 10^{-11} s$. The physical properties of the medium are: $\mu = 1.2566 \cdot 10^{-6} H/m$ and $\varepsilon = 8.8544 \cdot 10^{-12} F/m$.

Fig.3 shows the electric field intensity obtained at points A and B (see Fig.2), considering the two discussed MLPG formulations. Analytical time histories (Miles, 1961) are also depicted in Fig.3, highlighting the good accuracy of the numerical results, in spite of the poor MLPG discretization. In Fig.3a, results are depicted considering $m = 3$ (linear basis); whereas, in Fig.3b, results are depicted consider-

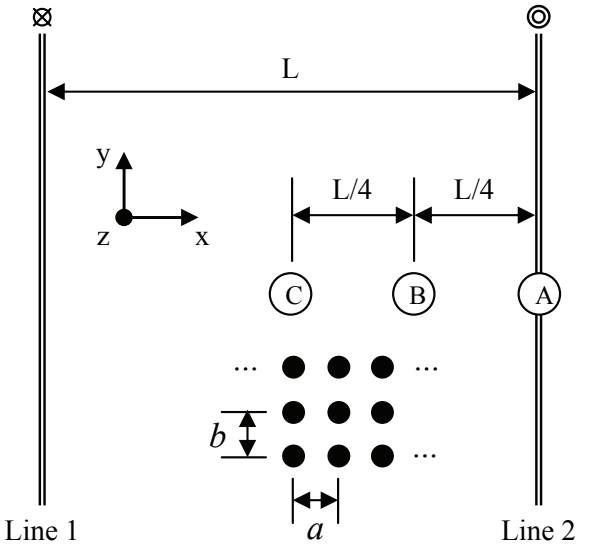

Figure 2: Sketch of the model: parallel lines of wires and spatial discretization.

ing $m = 6$ (quadratic basis – m is the number of terms in the definition of the basis vector $\mathbf{p}$). As can be observed, more accurate results are obtained once quadratic basis are considered, taking into account both MLPG formulations. In Fig.4, analogous results are presented, considering the computation of magnetic flux densities (secondary fields). Once again, good accuracy is observed.

It must be noticed that the example in focus is a very important benchmark since it represents a rather complex numerical computation (in spite of its geometrical and load simplicity) once there are successive reflections occurring at the model extremities and these multiple reflections can emphasize some numerical aspects, such as instabilities and excessive numerical damping.

6.2 Cylindrical lines of wires

In the present application, the electromagnetic fields surrounding two cylindrical lines of wires, carrying once again opposite time-linear currents, are studied. A sketch of the model and the adopted spatial discretization are depicted in Fig.5: the symmetry of the problem is taken into account and 1608 nodes are employed in the analyses (the geometry of the model is defined by $a = 1.0\,m$, $b = d = 0.25\,m$ and $R = 0.1\,m$). For the temporal discretization, the selected time-step is given by $\Delta t = 5 \cdot 10^{-11} s$. The physical properties of the medium are the same as in sub-

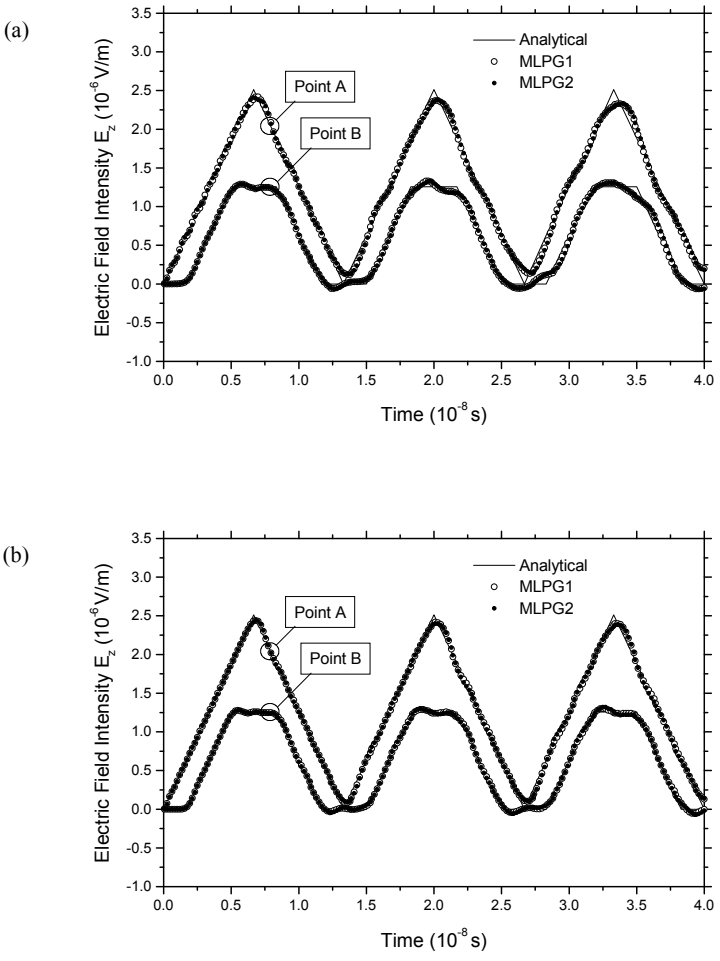

Figure 3: Time-history results for the electric field intensity at points A and B: (a) m= 3; (b) m= 6.

section 6.1.

Fig.6 shows the electric field intensity obtained at points A, B and C (see Fig.5), considering the two discussed MLPG formulations ($m = 6$) and boundary element techniques (Soares and Vinagre, 2008). In Fig.7, magnetic flux densities (secondary fields) are depicted. As can be observed, good agreement among the results is achieved.

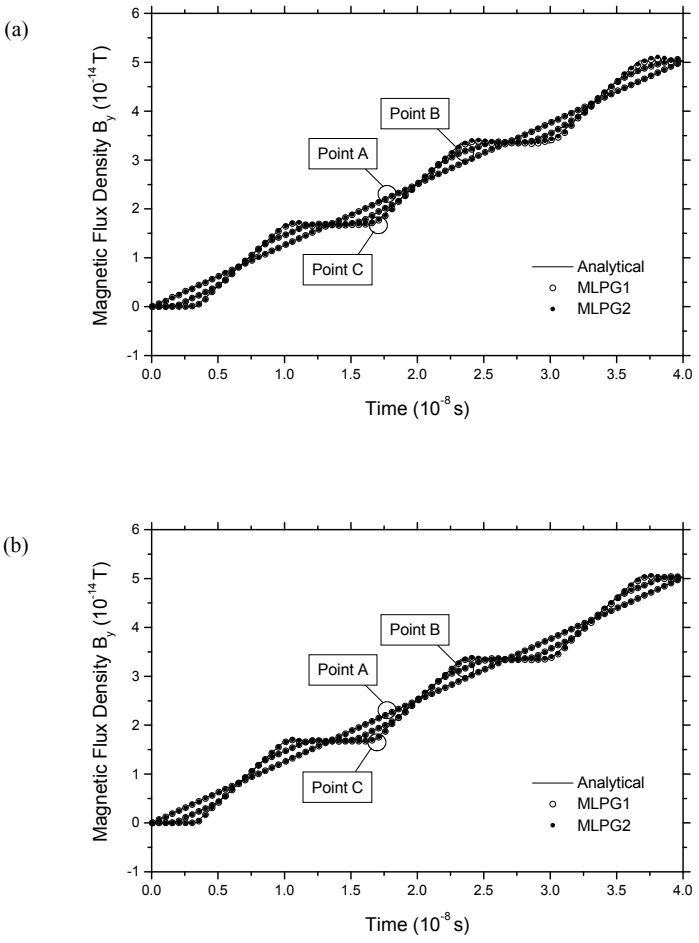

Figure 4: Time-history results for the magnetic flux density at points A, B and C: (a) m= 3; (b) m= 6.

7 Conclusions

Two MLPG formulations were presented to analyse electromagnetic wave propagation. In the first formulation, Heaviside step functions were adopted as the test functions, eliminating one domain integral of the local weak form equation. In the second formulation, Gaussian weight functions were the considered test functions, allowing eliminating boundary integrals along internal sub-domain contours. For both these formulations, a MLS interpolation scheme was adopted, rendering a matricial time-domain system of second order ordinary differential equations. This

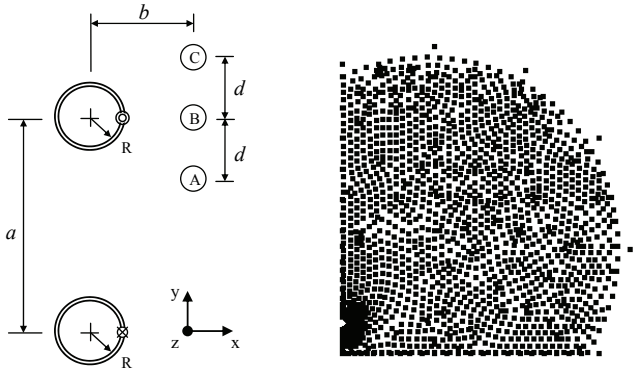

Figure 5: Sketch of the model: (a) cylindrical lines of wires and (b) spatial discretization.

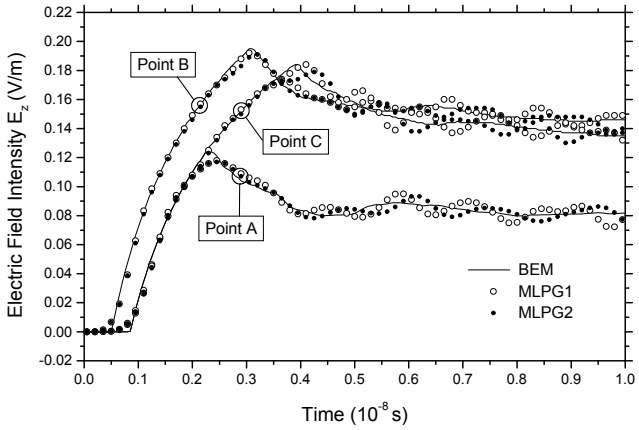

Figure 6: Time-history results for the electric field intensity at points A, B and C considering different numerical procedures.

system was analysed by time-marching procedures based on the Houbolt's method. Numerical results were provided at the end of the paper, illustrating the good accuracy of the proposed methodologies.

The meshless formulations presented here can be regarded as appropriate numerical tools to analyse electromagnetic fields: the usual difficulties related to mesh generation, as in some standard methods (such as the finite element method), are

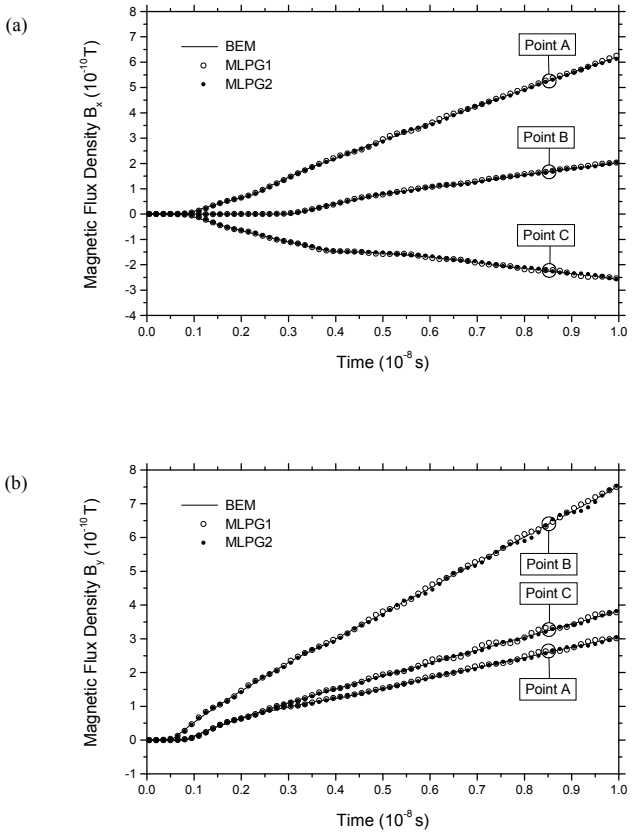

Figure 7: Time-history results for the magnetic flux density at points A, B and C considering different numerical procedures: (a) B_x; (b) B_y.

avoided; and continuous variation of spatial derivatives of primary fields is obtained, allowing the computation of secondary fields more effectively.

Acknowledgement: The financial support by CNPq (*Conselho Nacional de Desenvolvimento Científico e Tecnológico*) and FAPEMIG (*Fundação de Amparo à Pesquisa do Estado de Minas Gerais*) is greatly acknowledged.

References

Ala, G.; Francomano, E.; Tortofici, A.; Toscano, E.; Viola, F. (2007): Corrective meshless particle formulations for time domain Maxwell's equations, *Journal of Computational and Applied Mathematics* vol. 210, pp. 34–46.

Atluri, S.N. (2004): *The Meshless Method (MLPG) for Domain & BIE Discretizations*, Tech Science Press, Encino, CA.

Atluri, S.N.; Han, Z.D.; Rajendran, A.M. (2004): A new implementation of the meshless finite volume method, through the MLPG "Mixed" approach, *CMES: Computer Modeling in Engineering & Sciences* vol.6, pp. 491-513.

Atluri, S.N.; Han, Z.D.; Shen, S. (2003): Meshless local Petrov-Galerkin (MLPG) approaches for solving the weakly-singular traction & displacement boundary integral equations, *CMES: Computer Modeling in Engineering & Sciences* vol.4, pp. 507-517.

Atluri, S.N.; Shen, S.P. (2002): The meshless local Petrov-Galerkin (MLPG) method: A simple & less-costly alternative to the finite element and boundary element methods, *CMES: Computer Modeling in Engineering and Sciences* vol.3, pp. 11-51.

Atluri, S.N.; Shen S. (2002): *The Meshless Local Petrov-Galerkin (MLPG) Method*, Tech Science Press, Encino, CA.

Atluri, S.N.; Zhu, T. (1998): A New Meshless Local Petrov-Galerkin (MLPG) Approach in Computational Mechanics, *Computational Mechanics* vol.22, pp. 117-127.

Atluri, S.N.; Zhu, T. (2000): New concepts in meshless methods, *International Journal of Numerical Methods in Engineering* vol.47, pp. 537-556.

Clingoski, V.; Miyamoto, N.; Yamashita, H. (1998): Element-free Galerkin method for electromagnetic field computations, *IEEE Transactions on Magnetics* vol. 34, pp. 3236–3239.

Francomano, E.; Tortofici, A.; Toscano, E.; Ala, G.; Viola, F. (2009): On the use of a meshless solver for PDEs governing electromagnetic transients, *Applied Mathematics and Computation* vol. 209, pp. 42–51.

Guimaraes, F.G.; Saldanha, R.R.; Mesquita, R.C.; Lowther, D.A.; Ramirez, J.A. (2007): A meshless method for electromagnetic field computation based on the multiquadric technique, *IEEE Transactions on Magnetics* vol. 43, pp. 1281–1284.

Ho, S.L.; Yang, S.; Machado, J.M.; Wong, H.C. (2001): Application of a meshless method in electromagnetics, *IEEE Transactions on Magnetics* vol. 37, pp. 3198–3202.

Houbolt, J.C. (1950): A recurrence matrix solution for the dynamic response of elastic aircraft, *Journal of the Aeronautical Sciences* vol. 17, pp. 540–550.

Jin, J. (2002): *The finite element method in electromagnetics*, John Wiley & Sons, New York.

Lai, S.J.; Wang, B.Z.; Duan, Y. (2008): Meshless radial basis function method for transient electromagnetic computations, *IEEE Transactions on Magnetics* vol. 44, pp. 2288–2295.

Lee, K.M.; Li, Q.; Sun, H. (2006): Effects of numerical formulation on magnetic field computation using meshless methods, *IEEE Transactions on Magnetics* vol. 42, pp. 2164–2171.

Li, Q.; Lee, K.M. (2006): An adaptive meshless method for magnetic field computation, *IEEE Transactions on Magnetics* vol. 42, pp. 1996–2003.

Liu, X.; Wang, B.Z.; Lai, S. (2007): Element-free Galerkin method in electromagnetic scattering field computation, *Journal of Electromagnetic Waves and Applicatios* vol. 21, pp. 1915–1923.

Louai, F.Z.; Nait-Said, N.; Drid, S. (2007): Implementation of an efficient element-free Galerkin method for electromagnetic computation, *Engineering Analysis with Boundary Elements* vol. 31, pp. 191–199.

Manzin, A.; Bottauscio, O. (2008): Element-free Galerkin method for the analysis of electromagnetic-wave scattering, *IEEE Transactions on Magnetics* vol. 44 1366–1369.

Marechal, Y. (1998): Some meshless methods for electromagnetic field computations, *IEEE Transactions on Magnetics* vol. 34, pp. 3351–3354.

Marques, G.N.; Machado, J.M.; Verardi, S.L.L.; Stephany, S.; Preto, A.J. (2007): Interpolating EFGM for computing continuous and discontinuous electromagnetic fields, *COMPEL – The International Journal for Computing and Mathematics in Electrical and Electronic Engineering* vol. 26, pp. 1411–1438.

Miles, J.W. (1961): *Modern Mathematics for the Engineer* (E.F. Beckenbach, ed.), MacGraw-Hill, London.

Ni, G.Z.; Ho, S.L.; Yang, S.Y.; Ni, P.H. (2004): Meshless local Petrov-Galerkin method and its application to electromagnetic field computations, *International Journal of Applied Electromagnetics and Mechanics* vol. 19, pp. 111–117.

Parreira, G.F.; Silva, E.J.; Fonseca, A.R.; Mesquita, R.C. (2006) The element-free Galerkin method in three-dimensional electromagnetic problems, *IEEE Transactions on Magnetics* vol. 42, pp. 711–714.

Reutskiy, S.Y.; Tirozzi, B. (2004): A meshless boundary method for 2D problems of electromagnetic scattering from inhomogeneous bodies; H-polarized waves, *Journal of Quantitative Spectroscopy & Radiative Transfer* vol. 83, pp. 313–320.

Soares Jr., D. (2008): A Time-Domain FEM-BEM Iterative Coupling Algorithm to Numerically Model the Propagation of Electromagnetic Waves, *CMES: Computer Modeling in Engineering & Sciences* vol. 32, pp. 57-68.

Soares Jr., D. (2009): Numerical Modelling of Electromagnetic Waves by Explicit Multi-Level Time-Step FEM-BEM Coupling Procedures, *CMES: Computer Modeling in Engineering & Sciences* vol. 44, pp. 157-175.

Soares Jr., D.; Vinagre, M.P. (2008): Numerical Computation of Electromagnetic Fields by the Time-Domain Boundary Element Method and the Complex Variable Method, *CMES: Computer Modeling in Engineering & Sciences* vol. 25, pp. 1-8.

Viana, S.A.; Rodger, D.; Lai, H.C. (2004): Meshless local Petrov-Galerkin method with radial basis functions applied to electromagnetics, *IEEE Proceedings – Science Measurement and Technology* vol. 151, pp. 449–451.

Xuan, L.; Zeng, Z.W.; Shanker, B.; Udpa, L. (2004) Element-free Galerkin method for static and quasi-static electromagnetic field computation, *IEEE Transactions on Magnetics* vol. 40, pp. 12–20.

Young, D.L.; Chen, C.S.; Wong, T.K. (2005): Solution of Maxwell's equations using the MQ method, *CMC: Computers Material & Continua* vol. 2, pp. 267–276.

Zhao, M.L.; Nie, Y.F. (2008): A Study of Boundary Conditions in the Meshless Local Petrov-Galerkin (MLPG) Method for Electromagnetic Field Computations, *CMES: Computer Modeling in Engineering & Sciences* vol. 37, pp. 97-112.